Effects of a finite size reflecting disk in sound power measurements

Jiaxin Zhong[1], Jiancheng Tao[1a)], Feng Niu[1,2], Xiaojun Qiu[3]

[1] Key Laboratory of Modern Acoustics and Institute of Acoustics, Nanjing University, Nanjing, China

[2] Department of Mechanics and Acoustics, National Institute of Metrology, Beijing, China

[3] Centre for Audio, Acoustics and Vibration, Faculty of Engineering and IT, University of Technology Sydney, Sydney, Australia

a) Author to whom correspondence should be addressed; electric mail: jctao@nju.edu.cn.

ABSTRACT

In practical sound power measurements in an anechoic room, a baffle sometimes has to be used to support the sound source under test so that the anechoic room can be used as a hemi-anechoic room by laying a reflecting plane. To understand the effects of a finite size reflecting plane on measurements quantitatively, this paper investigates the effects of a disk on sound power measurements by formulating an exact solution to the problem based on the spheroidal wave functions. Three practical measurement cases are considered and the correction terms for the cases are presented based on numerical simulations. Experiments are conducted to validate the analytical solutions and numerical results.

1. Introduction

Sound power level (SWL) is an important parameter for characterizing a noise source and can be determined based on the sound pressure method [1], sound intensity method [2] or other indirect methods [3] in practical measurements. SWL measurements of a sound source can be conducted in an anechoic room or a hemi-anechoic room (free field over an infinite size reflecting plane) based on the sound pressure method [4]. In some practical situations, sound sources need a baffle to support them when they are measured in a full anechoic room, and a full anechoic room sometimes has to be used as a hemi-anechoic room by laying a reflecting plane. Therefore, the effects of a finite size reflecting plane on measurements need to be quantitatively investigated, which is the aim of this technical note.

The image source method has been used to analyze the effects of the infinite size reflecting plane in sound power measurements [5, 6]. However, when the size of reflecting plane is comparable to the wavelength of sound, considerable error occurs in the power estimation, so further study is needed [7]. A finite size circular disk is often used in an anechoic room as a reflecting plane, so the sound reflection and scattering from a circular disk is calculated in the note to understand the effects of a finite size reflecting plane on measurements.

A circular disk was first considered as a degenerate oblate spheroid in acoustics in 1933 [8], then Bouwkamp developed the diffraction theory by circular disks in the oblate

spheroidal coordinate system in 1950 [9], and an analytical solution of the Green's function with an oblate rigid boundary can be found in [10]. The solution involves two special functions named as radial and angular spheroidal wave functions which are difficult to compute accurately in 1970s. Based on the asymptotic forms of these two functions, Lauchle studied the far field directivity of a monopole above a disk and conducted experiments using a loudspeaker in 1979 [11].

In recent years, with the progress of computation methods and resources, some software or codes are available for calculating these two functions accurately [12,13]. Based on that, Adelman computed near field sound pressure scattered by a rigid disk in 2014 [14]. In our previous work, a circular disk was introduced to support a sound source in free space and the measurement correction term was simulated and computed according to the computation methods [15]. However, little attention has been paid to the calculation of sound power output of sound sources near a finite size disk.

This paper derives the exact solutions to three practical measurement cases based on the spheroidal wave functions. Three cases include: (1) a supporting baffle has to be used in measurements in a full anechoic room and the sound pressure on spherical measurement surface is obtainable; (2) a supporting baffle has to be used in measurements in a full anechoic room and only the sound pressure on the hemi-spherical measurement surface above the disk is obtainable (this case occurs in practice when it is difficult to install

microphones below the wire-meshed floor in a full anechoic room or there are not enough microphones); and (3) an anechoic room is used to simulate the environment in a hemi-anechoic room by laying a finite size rigid disk on the wire-meshed floor. The correction terms for the cases are provided based on simulations, and experiments are conducted to validate the analytical and numerical results.

2. Theory

The model of sound power measurements is shown in Fig. 1, where a monopole is placed on the axis of a finite size rigid disk with a radius of a, and the acoustic center of the source locates h meters above the disk. Measuring microphones are installed on a spherical or hemi-spherical measurement surface to obtain the sound pressure. The sound power of the noise source is determined according to the surface averaged sound pressure as [4]

$$L_{\mathrm{W,m}} = 10\lg\left(\frac{1}{N}\sum_{n=1}^{N}10^{0.1L_{\mathrm{p},n}}\right)+10\lg\left(\frac{S}{S_0}\right), \tag{1}$$

where $L_{\mathrm{W,m}}$ denotes the measured SWL, N is the total number of measuring microphones, $L_{\mathrm{p},n}$ is the sound pressure level (SPL) at the nth microphone, $S = 4\pi R^2$ or $2\pi R^2$ for the spherical or hemi-spherical measurement surface respectively, R is the radius of measurement surface, and $S_0 = 1\ \mathrm{m}^2$.

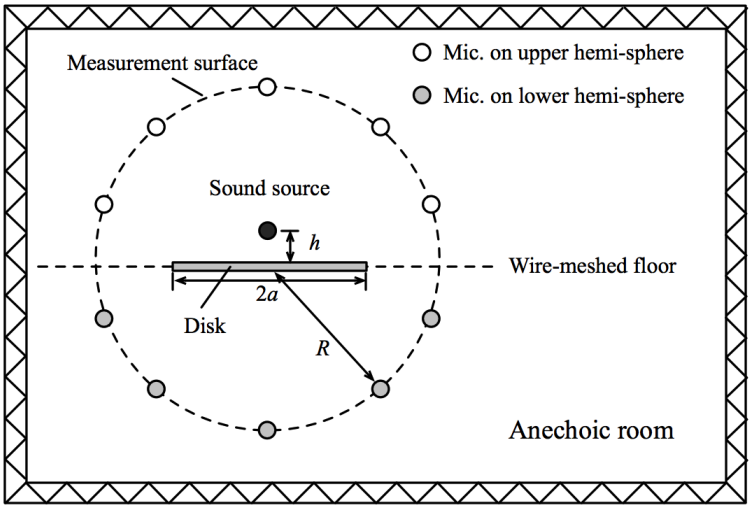

Fig. 1. Sketch of sound power measurements with a finite size rigid disk based on the sound pressure method in a full anechoic room

The total radiated sound with the disk, p_{disk}, is the superposition of the direct sound from the monopole source and the scattering sound due to the disk respectively. The governing equation of sound field can be solved by using the boundary condition on the disk surface,

$$\left.\frac{\partial p_{\text{disk}}}{\partial \xi}\right|_{\xi=\xi_b} = 0, \tag{2}$$

where the disk surface is assumed to be acoustically hard, ξ is the radial oblate spheroidal coordinate in the oblate spheroid coordinate system, ξ_b represents the boundary surface, and the oblate coordinates (η, ξ, φ) are related to the Cartesian coordinates (x, y, z) by [10]

$$\begin{aligned} x &= a\sqrt{(1-\eta^2)(1+\xi^2)}\cos\varphi \\ y &= a\sqrt{(1-\eta^2)(1+\xi^2)}\sin\varphi. \\ z &= a\eta\xi \end{aligned} \tag{3}$$

When the radial coordinate $\xi = 0$, the oblate represents an infinitely thin disk with a radius of a on the plane $z = 0$ in the Cartesian coordinate system [10]. When ξ is sufficiently large, the oblate tends to be a sphere and the angular coordinate η and ξ can be related to the spherical

coordinates (r, θ, φ) as $a\xi \to r$ and $\eta \to \cos\theta$, where r is the radial coordinate, θ is zenith angle and φ is the azimuth angle [10].

The total sound pressure solution at an arbitrary field point (η, ξ, φ) is [10]

$$p_{\text{disk}}(\eta,\xi,\varphi)=\frac{\rho\omega kQ}{4\pi}\sum_{m=0}^{\infty}\sum_{n=m}^{\infty}\frac{2\varepsilon_m}{N_{mn}(-\text{j}ka)}S_{mn}(-\text{j}ka,\eta)S_{mn}(-\text{j}ka,\eta_{\text{s}})\cos[m(\varphi-\varphi_{\text{s}})] \times\left[\begin{array}{c} R_{mn}^{(1)}(-\text{j}ka,\text{j}\xi_{<})R_{mn}^{(3)}(-\text{j}ka,\text{j}\xi_{>}) \\ -\dfrac{R_{mn}^{(1)'}(-\text{j}ka,\text{j}\xi_{\text{b}})}{R_{mn}^{(3)'}(-\text{j}ka,\text{j}\xi_{\text{b}})}R_{mn}^{(3)}(-\text{j}ka,\text{j}\xi)R_{mn}^{(3)}(-\text{j}ka,\text{j}\xi_{\text{s}}) \end{array}\right], \tag{4}$$

where the notations adopted follow that used by Flammer [10], ρ is the density of air, ω is the angular frequency of the sound emitted by the source with real volume velocity Q and the harmonic term $\exp(-\text{j}\omega t)$ is omitted, k is the wavenumber, $\varepsilon_m = 1$ for $m = 0$ and $\varepsilon_m = 2$ for $m \neq 0$. The oblate wave function $S_{mn}(-\text{j}ka, \eta)$ is the angular oblate spheroidal wave function and $N_{mn}(-\text{j}ka)$ is the normalization factor of $S_{mn}(-\text{j}ka, \eta)$. $R_{mn}^{(i)}(-\text{j}ka, \text{j}\xi)$ and $R_{mn}^{(i)'}(-\text{j}ka, \text{j}\xi)$ represent the ith kind of the radial oblate spheroidal wave functions and their derivatives with respect to ξ, $i = 1, 3$ [10], ξ_{b} is the radial coordinate of the boundary ($\xi_{\text{b}} = 0$ for a disk), (η_{s}, ξ_{s}, φ_{s}) are the oblate coordinates of the source, $\xi_{<} = \min(\xi, \xi_{\text{s}})$ and $\xi_{>} = \max(\xi, \xi_{\text{s}})$.

In the far filed where ξ is sufficiently large, the radial functions $R_{mn}^{(3)}(-\text{j}ka, \text{j}\xi)$ have asymptotic values as $(kr)^{-1}\exp[\text{j}kr - \text{j}\pi(n + 1)/2]$ [10], and Eq. (4) can be written in the spherical coordinate system as

$$p_{\text{disk,far}}(r,\theta,\varphi)=\frac{\rho\omega Q}{4\pi r}e^{\text{j}kr}\sum_{m=0}^{\infty}\sum_{n=m}^{\infty}\frac{2\varepsilon_m(-\text{j})^{n+1}}{N_{mn}(-\text{j}ka)}S_{mn}(-\text{j}ka,\cos\theta)S_{mn}(-\text{j}ka,\eta_{\text{s}}) \times\cos[m(\varphi-\varphi_{\text{s}})]\left[R_{mn}^{(1)}(-\text{j}ka,\text{j}\xi_{\text{s}})-\frac{R_{mn}^{(1)'}(-\text{j}ka,\text{j}\xi_{\text{b}})}{R_{mn}^{(3)'}(-\text{j}ka,\text{j}\xi_{\text{b}})}R_{mn}^{(3)}(-\text{j}ka,\text{j}\xi_{\text{s}})\right]. \tag{5}$$

The sound power can be calculated using the radiation impedance and the strength of the acoustic source. By substituting Eq. (4) into the sound power formulation $W = 0.5\mathrm{Re}(Z_s)Q^2$, where Z_s is the radiation impedance of the source at (η_s, ξ_s, φ_s) and related to the sound pressure as $Z_s = p_{\mathrm{disk}}(\eta_s, \xi_s, \varphi_s)/Q$ [3], the sound power of the source with the disk can be expressed by

$$W_{\mathrm{disk}} = \frac{\rho\omega k Q^2}{8\pi}\sum_{m=0}^{\infty}\sum_{n=m}^{\infty}\frac{2\varepsilon_m}{N_{mn}(-\mathrm{j}ka)}\left[S_{mn}(-\mathrm{j}ka,\eta_s)\right]^2 \times\left|R_{mn}^{(1)}(-\mathrm{j}ka,\mathrm{j}\xi_s)-\frac{R_{mn}^{(1)'}(-\mathrm{j}ka,\mathrm{j}\xi_b)}{R_{mn}^{(3)'}(-\mathrm{j}ka,\mathrm{j}\xi_b)}R_{mn}^{(3)}(-\mathrm{j}ka,\mathrm{j}\xi_s)\right|^2. \tag{6}$$

Although the solution of the sound pressure in Eq. (4) was published by many researchers, the solution of sound power for a disk in Eq. (6) has not been found in literatures. Consider that the monopole source is located on the disk axis in Fig. 1, the mode parameter $m = 0$ and the angular coordinate $\eta = 1$, the sound power with the disk can be simplified as

$$W_{\mathrm{disk}} = \frac{\rho\omega k Q^2}{8\pi}\sum_{n=0}^{\infty}\frac{2}{N_{0n}(-\mathrm{j}ka)}[S_{0n}(-\mathrm{j}ka,1)]^2 \times\left|R_{0n}^{(1)}(-\mathrm{j}ka,\mathrm{j}h/a)-\frac{R_{0n}^{(1)'}(-\mathrm{j}ka,\mathrm{j}0)}{R_{0n}^{(3)'}(-\mathrm{j}ka,\mathrm{j}0)}R_{0n}^{(3)}(-\mathrm{j}ka,\mathrm{j}h/a)\right|^2. \tag{7}$$

If the monopole is located on the disk center, the distance $h = 0$, and Eq. (7) can be further simplified using the Wronskian relation as

$$W_{\mathrm{disk}} = \frac{\rho\omega k Q^2}{8\pi}\sum_{n=0}^{\infty}\frac{2}{N_{0n}(-\mathrm{j}ka)}\left|\frac{S_{0n}(-\mathrm{j}ka,1)}{R_{0n}^{(3)'}(-\mathrm{j}ka,\mathrm{j}0)}\right|^2. \tag{8}$$

The sound power radiated into the upper half-space above the disk cannot be directly obtained using the radiation impedance. An alternative method is to integrate the sound intensity travelling out a hemi-spherical surface in the upper half-space. The sound intensity

in the far field can be approximately calculated by dividing the squared sound pressure by air density and sound speed. So, the discrete summarization form of the sound power in the upper half-space is

$$W_{\text{disk,above}} = \lim_{L\to\infty} \frac{\pi R^2}{\rho c L} \sum_{l=1}^{L} | p_{\text{disk,far}} (R, \theta_l, \varphi_l) |^2 , \tag{9}$$

where L is the number of discrete field points, R is the radius of the hemi-spherical surface, $p_{\text{disk,far}}(R, \theta_l, \varphi_l)$ is the sound pressure at the center (R, θ_l, φ_l) of the lth area element on the hemi-spherical surface.

The sound power of the source without and with an infinite size reflecting plane is well known as [16]

$$W_{\text{free}} = \frac{\rho \omega k Q^2}{8\pi}, \tag{10}$$

$$\text{and} \quad W_{\text{inf}} = \frac{\rho \omega k Q^2}{8\pi} [1 + \text{sinc}(2kh)], \tag{11}$$

where $\text{sinc}(x) = \sin(x)/x$, and h is the distance between the source and the reflecting plane.

For the convenience of the analysis, three types of correction terms are defined as the following,

$$C_1 = 10 \lg(W_{\text{disk}} / W_{\text{free}}), \tag{12}$$

$$C_2 = 10 \lg(W_{\text{disk,above}} / W_{\text{disk}}), \tag{13}$$

$$\text{and} \quad C_3 = 10 \lg(W_{\text{free}} / W_{\text{inf}}) . \tag{14}$$

In case 1, a supporting baffle has to be used in measurements in a full anechoic room and the sound pressure on spherical measurement surface is obtainable, the correction term is C_1. In case 2, a supporting baffle has to be used in measurements in a full anechoic room and

only the sound pressure on the hemi-spherical measurement surface above the disk is obtainable, the correction term is $C_1 + C_2$. In case 3, an anechoic room is used to simulate the environment of a hemi-anechoic room by laying a finite size rigid disk on the wire-meshed floor, the correction term is $C_1 + C_2 + C_3$. The final SWL after corresponding corrections is

$$L_{\mathrm{W}} = L_{\mathrm{W,m}} - \sum_{i=1}^{N_{\mathrm{c}}} C_i,\ N_{\mathrm{c}} = 1, 2, 3, \tag{15}$$

where N_{c} represents the number of measurement case.

3. Simulations and discussions

A MATLAB program was developed to compute the numerical results. The subroutines of spheroidal wave functions were partly referred to the code provided by Zhang (Chap. 15 in [12]) and was modified for $\xi = 0$ (Sec. 4.6.2 in [10]). In the simulations, the sound source is placed on the axis of the disk, thus $m = 0$ and $\varphi = \varphi_{\mathrm{s}} = 0$. Fig. 2 shows the calculated sound pressure level at some randomly chosen locations by using Eq. (4) and the boundary element method (BEM) simulation software (LMS Virtual.Lab Acoustics 12.0 [17]). The disk radius a is 0.5 m, and the source height h is 0.1 m. The source strength $\rho\omega Q/(\mathrm{j}4\pi)$ is set as 1 kg/s^2 for all frequencies. Fig. 2 shows that the maximal difference between the theoretical results and numerical results obtained by BEM is less than 0.1 dB from 63 Hz to 800 Hz.

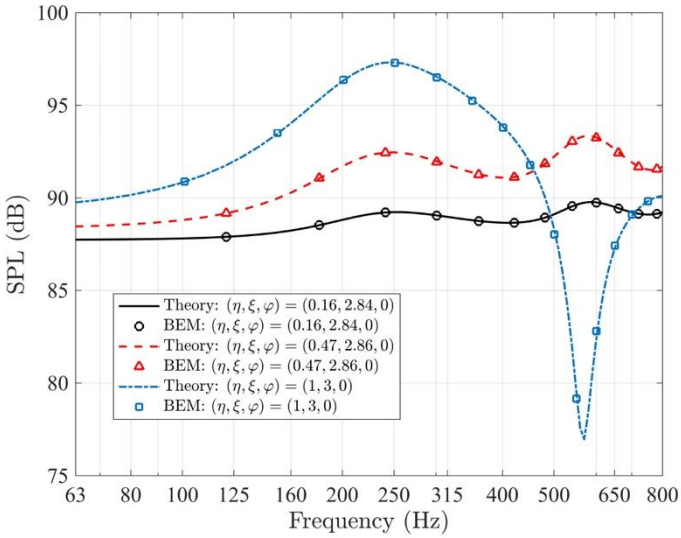

Fig. 2. Calculated sound pressure level at 3 randomly selected field points using the theoretical solution and the BEM simulation (a = 0.5 m, h = 0.1 m, $\rho\omega Q/(\mathrm{j}4\pi)$ = 1 kg/s^2)

If a supporting baffle has to be used in a full anechoic room measurement, the correction term is C_1. Fig. 3 shows the correction terms (the ratio of sound power with and without the disk, i.e. C_1) for different disk radii and source heights under this case. It can be seen that the correction term is nearly 0 dB when the disk radius is sufficiently small or when the source height is sufficiently large; however, the correction term fluctuates significantly when the disk radius and source height are comparable to the wavelength λ.

Fig. 3(a) shows that for h = 0, the correction term increases to about 4.0 dB with the disk radius when a is below 0.35λ and then converges to 3.0 dB. For h = 0.5λ, the correction term decreases to about −1.2 dB with the disk radius when a is below 0.36λ, and then converges to 0 dB. For h = 1.5λ, the correction term has a similar variation trend as that of h = 0.5λ but with smaller and slower fluctuations. Fig. 3(b) shows that the correction term decreases with

the source height first and then converges to 0 dB regardless of the disk radius. The maximal correction term at h = 0 is about 1.5 dB, 4.0 dB and 3.0 dB respectively when a = 0.2λ, 0.35λ and 1.5λ, while the minimal correction term is about −0.2 dB, −1.7 dB and −1.4 dB when h is around 0.53λ, 0.43λ and 0.36λ respectively.

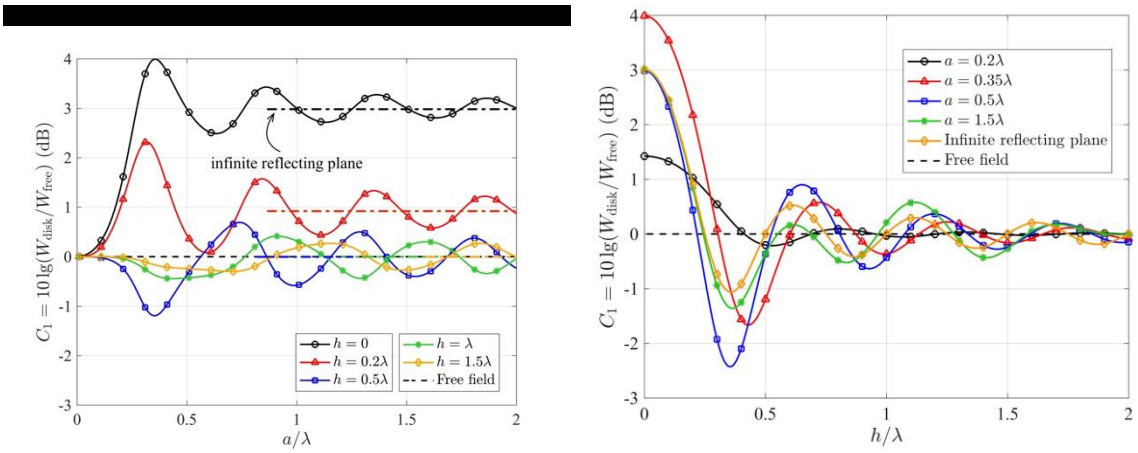

(a) (b)

Fig. 3. The correction terms in case 1 as a function of (a) disk radius a with different source height h; (b) source height h with different disk radius a

Take h = 0 as an example to explain the correction term fluctuation. When the sound is generated from the center of the disk, the sound waves traveling out radially along the surface of the disk meet with an abrupt change of curvature at the edge of the disk [11]. The wave reflects from the medium at the edges in antiphase, relative to the source point and the sound pressure of reflected wave is proportional to jQexp(j2ka) [11]. Because the total radiated sound is the superposition of the direct and reflected sound and the sound source is located on

the disk center, the change of the real part of radiation impedance is proportional to $-\mathrm{sinc}(2ka)$. The fluctuations of total radiation power are then caused by the behavior of function $-\mathrm{sinc}(2ka)$ according to the sound power formulation $W = 0.5\mathrm{Re}(Z_s)Q^2$. Therefore, the peaks and valleys of the curves with $h = 0$ correspond to the valleys and peaks of the function $\mathrm{sinc}(2ka)$ respectively. The first valley of $\mathrm{sinc}(2ka)$ appears when $2ka \approx 1.4\pi$, so the first peak of the curve $h = 0$ in Fig. 3(a) occurs at $a \approx 0.35\lambda$.

If measuring microphones cannot be installed under the rigid disk in the full anechoic room, the correction term is $C_1 + C_2$. Fig. 4 shows the correction terms for different disk radii and source heights under this case. The curves in Fig. 4 have the similar trends as those in Fig. 3, except that the values of curves in Fig. 4 are generally smaller than those in Fig. 3. This is because the ratio of sound power above the disk to the total power is always less than 1. In general, the larger the radius a is, the larger this power ratio will be. Therefore the level differences between curves in Fig. 3(a) and Fig. 4 (a) decreases with the radius a. Particularly, when a is nearly 0, the sound power above the disk is half of the total sound power, which means $C_1 + C_2 = 0 + 10\lg(0.5) = -3$ dB. Fig. 4(b) shows that the minimal correction term is −6.9 dB when $a = 0.35\lambda$ and $h = 0.41\lambda$, and its absolute value is larger than the maximum of the correction terms, 4.0 dB, when $a = 0.35\lambda$ and $h = 0$ in case 1. For other disk radii or source heights, the difference between the maximal and minimal value of the correction terms in case 2 are generally greater than those in case 1.

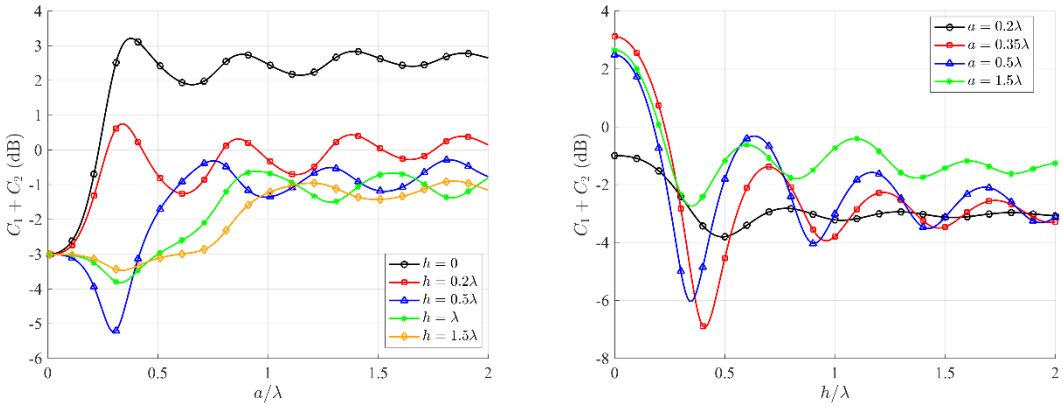

(a) (b)

Fig. 4. The correction terms in case 2 as a function of (a) disk radius *a* with different source height *h*; (b) source height *h* with different disk radius *a*

When a full anechoic room is used to simulate the acoustic environment of a hemi-anechoic room by laying a finite size rigid disk, the correction term is $C_1 + C_2 + C_3$. Fig. 5 shows the correction terms for different disk radii and source heights under this case. The correction term is generally less than 0 dB which means the measured SWL under with this configuration is less than the desired SWL in a hemi-anechoic room. Fig. 5(a) shows that if the source height can be considered as 0, the correction term could be less than 1.1 dB when the disk radius is larger than 0.28λ. When the disk radius decreases from 0.28λ, the correction term decreases rapidly and becomes −6 dB when disk radius is nearly 0. This implies that the measured sound power by using a small disk to simulate the acoustic environment of a hemi-anechoic room is 6 dB lower that than that obtained in a real hemi-anechoic room in the low frequency range. Fig. 5(b) shows that the correction term is within the range between −1.7 dB

and −0.4 dB when the disk radius approaches 1.5λ, which means that the fluctuations are moderately small regardless of the source heights.

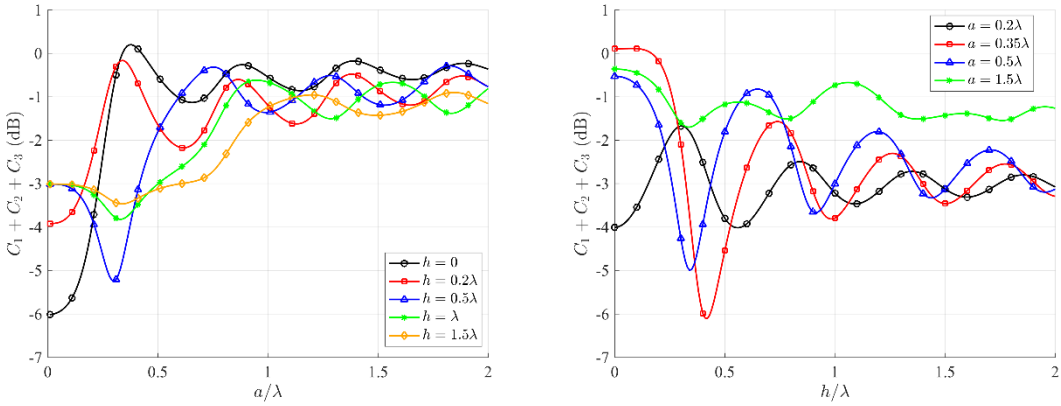

(a) (b)

Fig. 5. The correction terms in case 3 as a function of (a) disk radius *a* with different source height *h*; (b) source height *h* with different disk radius *a*

4. Experiments

The ratio of sound power radiated by a monopole with a disk to that without disk (C_1), the ratio of sound power radiated into upper half-space above the disk to the total power (C_2) and the ratio of sound power radiated above an infinite size reflecting plane to that in free field (C_3) were measured by experiments. Fig. 6 shows the experimental setup in a full anechoic room in Nanjing University with the dimension of 11.4 m × 7.8 m × 6.7 m and a hemi-anechoic room in National Institute of Metrology (China) with the dimension of 13.2 m × 10.0 m × 7.2 m. The low frequency volume source VSS 058 made by BSWA Technology Co Ltd. is employed as the monopole sound source [18]. The frequency range of the volume

source is 50 ~ 800 Hz and the source strength can be calculated using the internal microphone inside the source. The acoustic center of the source is on the axis of the source and about 55 cm above the bottom shell. A wooden plate with a radius of 0.5 m and a thickness of 1.8 cm is used as the rigid disk. The surface density of the disk is about 15.30 kg/m^2. According to the Fig. 3 in [7], in such a case, the ratio of sound power reflected from the disk to the total sound power radiated from the sound source is larger than 96.6% above 100 Hz.

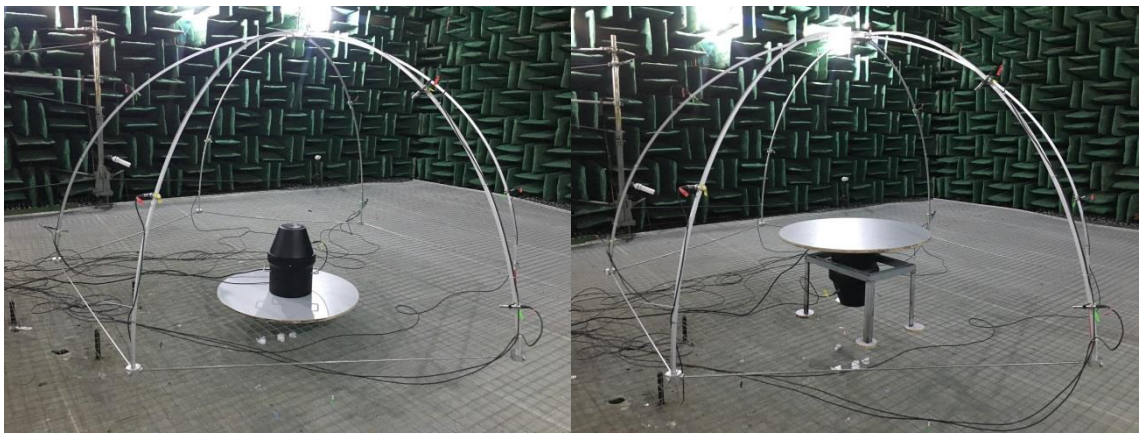

(a) (b)

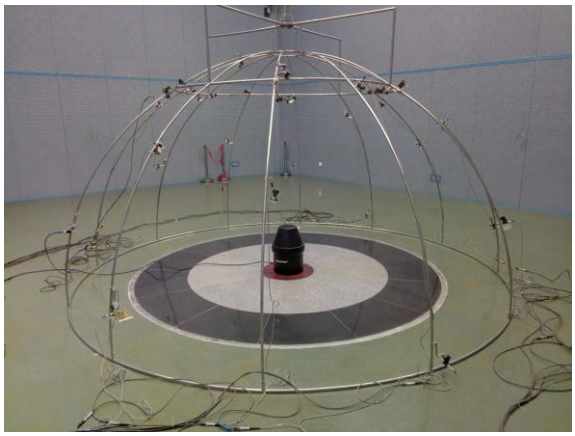

(c)

Fig. 6. Experimental setup of the volume source and rigid disk in a full anechoic room: (a) the source and the disk are placed upward; (b) the source and the disk are placed downward. (c) Experimental setup of the volume source in a hemi-anechoic room

The total sound power in the full anechoic room is determined according to Eq. (1) using the sound pressure at 40 measuring microphones on a spherical surface (with a radius of 1.5 m), and the sound pressure at 20 measuring microphones below the disk are obtained by reversing the sound source together with the disk as shown in Fig. 6(b). The sound pressure at measuring microphones was sampled with a B&K PULSE system and the FFT analyzer in PULSE LabShop 12.6.1 was used to obtain the FFT spectrum. The frequency span was set to 1.6 kHz with 1600 lines and the averaging type is linear with 66.67% overlap and 30 seconds duration. To obtain the SWL in the upper half space, 20 measuring microphones were installed on the hemi-spherical frame as shown in Fig. 6(a). Only 10 microphones could be mounted on the hemispherical frame adopted in the anechoic room at a time, therefore two 10-point measurements were conducted for the 20-point measurement. The total sound power in the hemi-anechoic room was determined in a similar way on a hemi-spherical surface (with a radius of 2 m) as shown in Fig. 6(c). The locations of measuring microphones on the hemi-sphere frame are chosen according to Table E.1 – Microphones positions (general case) in ISO 3745 in the measurements [4].

The three individual correction terms as well as the total correction terms for cases 1, 2 and 3 are shown in Fig. 7, where the experimental results agree reasonably well with the

theoretical results. The differences between 200 – 270 Hz and 500 – 635 Hz might be caused by the acoustical properties of the real disk, the measurement errors and the directivity pattern of the sound source. The measured correction terms for the three cases at 50 Hz are nearly 0 dB, −3 dB and −6 dB respectively. The minima of measured correction terms appear around the frequency of 260 Hz, where the reflecting plane radius 0.5 m approximately equals 0.35 wavelength. The correction terms can be large. For example, the theoretical correction term for case 2 at 260 Hz shown in Fig. 7 (b) is −7.0 dB and the measured value is −5.3 dB. It is clear that the effect of the finite size baffle should not be neglected and the proposed correction terms can be used for the accurate measurements of the sound power.

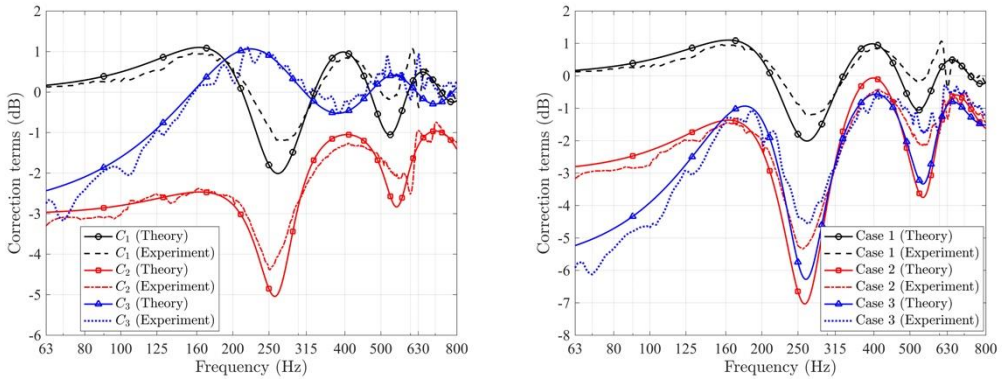

(a) (b)

Fig. 7. Comparisons of the correction terms calculated by theory and obtained by experiments for (a) C_1, C_2 and C_3 (b) Cases 1, 2 and 3

5. Conclusions

This paper investigates the effects of a finite size reflecting disk on sound power

measurements by formulating an exact solution of sound power output based on the spheroidal wave functions. Three practical measurement cases are considered and the correction terms are presented based on the numerical simulations and validated by the experiments. It is found that the measurement error can be up to 7.0 dB without correction and the measured sound power level is generally less than the desired one when a full anechoic room is used to simulate the acoustic environment in a hemi-anechoic room by laying a finite size circular reflecting plane. Future work includes considering the effects of the locations of acoustic source deviated from the axis of the disk and the directivity of sources in the proposed models.

Acknowledgements

This research was supported by the National Science Foundation of China (11474163) and under the Australian Research Council's Linkage Projects funding scheme (LP140100740).

References

[1] Hickling R, Lee P, Wei W. Investigation of integration accuracy of sound-power measurement using an automated sound-intensity system. Appl Acoust 1997;50(2):125−40.

[2] Fahy FJ. International standards for the determination of sound power levels of sources

using sound intensity measurement: an exposition. Appl Acoust 1997;50(2):97−109.

[3] Bote JLS, Gil JS, Ballesta FA, Morales LPG. Procedure for determination of sound power levels of direct-radiator loudspeakers in the low-frequency range using the sound pressure within the system enclosure. Appl Acoust 2015;96:75−82.

[4] ISO 3745. Acoustics — Determination of sound power levels and sound energy levels of noise sources using sound pressure — Precision methods for anechoic rooms and hemi-anechoic rooms; 2012.

[5] Suzuki H, Nakamura M, Tichy J. An accuracy evaluation of the sound power measurement by the use of the sound intensity and the sound pressure methods. Acoust Sci Tech 2007;28(5):319−27.

[6] Lim KM. Experimental investigation of the power radiated by a monopole above a reflected plane. Appl Acoust 1981;15:283–5.

[7] Yamada K, Takahashi H, Horiuchi R. Theoretical and experimental investigation of sound power transmitting through reflecting plane with low surface density in the calibration of reference sound sources. Acoust Sci Tech 2015;36(4):374–6.

[8] Kotani MI. An acoustic problem relating to the theory of the Rayleigh disc. Proc Phys Math Soc (Japan) 1993;15(1):30-57.

[9] Bouwkamp CJ. On the freely vibrating circular disk and the diffraction by circular disks and apertures. Physica 1950;16(1):1–16.

[10] Flammer C. Spheroidal wave functions. Stanford University Press, Stanford, CA; 1957.

[11] Lauchle GC. Radiation of sound from a small loudspeaker located in a circular baffle. J Acoust Soc Am 1975;57(3):543−9.

[12] Zhang S, Jin J. Computation of special functions. Wiley, New York; 1996;Chap 15.

[13] Adelman R, Gumerov NA, Duraiswami R. Software for computing the spheroidal wave functions using arbitrary precision arithmetic. arXiv 2014;1408.0074.

[14] Adelman R, Gumerov NA, Duraiswami R. Semi-analytical computation of acoustic scattering by spheroids and disks. J Acoust Soc Am 2014;136(6):EL405–10.

[15] Zhong J, Tao J, Qiu X. Effects of the finite circular baffle size on the sound power measurement. Proceedings of Inter-Noise17, Hong Kong, China; 2017.

[16] Waterhouse RV. Output of a sound source in a reverberation chamber and other reflecting environments. J Acoust Soc Am 1958;30(1):4–13.

[17] Siemens PLM Software. LMS Virtual.Lab. Product Brochure 2014;4−5.

[18] BSWA Technology Co Ltd. VSS 058 Low Frequency Volume Source. Product Brief 2016;1−2.